IOPscience iopscience.iop.org

Home Search Collections Journals About Contact us My IOPscience

The effect of electric field on intrasubband and intersubband transitions via interface phonons in GaAs-AlAs quantum wells

This article has been downloaded from IOPscience. Please scroll down to see the full text article.

1992 J. Phys.: Condens. Matter 4 9831

(http://iopscience.iop.org/0953-8984/4/49/011)

View the table of contents for this issue, or go to the journal homepage for more

Download details:
IP Address: 171.66.16.96
The article was downloaded on 11/05/2010 at 00:59

Please note that terms and conditions apply.

J. Phys.: Condens. Matter 4 (1992) 9831–9842. Printed in the UK

The effect of electric field on intrasubband and intersubband transitions via interface phonons in GaAs–AlAs quantum wells

Gerald Weber

Departamento de Física, Instituto de Ciências Exatas, Universidade Federal de Minas Gerais, Caixa Postal 702, 30161-970 Belo Horizonte, Minas Gerais, Brazil†

Received 12 May 1992, in final form 1 July 1992

Abstract. We calculate the scattering rates for intrasubband and intersubband transitions in GaAs–AlAs quantum wells due to interface phonons with an applied longitudinal electric field. The electron–interface-phonon (Fröhlich) Hamiltonian used is that obtained from the Fuchs–Kliewer slab model, and the electron envelope wavefunction under the influence of an electric field parallel to the growth direction is obtained by a variational method. The usual selection rules for these transitions break down and the scattering rates are found to increase significantly when an electric field is applied. These scattering rates may even become the dominant scattering mechanism for large quantum wells and sufficiently high fields. We observe also that this change in scattering rates has an important dependence on the interface-phonon dispersion.

1. Introduction

Interface-phonon modes in quantum wells and superlattices has become a subject of great interest in the past few years. Together with confined phonon modes they form the phonon modes which arise from the introduction of low dimensionality in semiconductor physics. The phonon modes were observed experimentally and their existence is well accepted. Sood *et al* [1], in 1985, observed interface (IF) phonons in GaAs–AlAs superlattices in Raman scattering measurements. Interface phonons in GaAs–AlGaAs superlattices were observed by Lambin *et al* [2] using high-resolution electron-energy-loss spectroscopy. Maciel *et al* [3], and Arora *et al* [4] observed GaAs confined and interface phonons, also in GaAs–AlGaAs superlattices, using resonant Raman scattering techniques. There are several papers on short-period GaAs–AlAs superlattices [5] and GaSb–AlSb strained-layer superlattices [6].

The influence of an electric field on the scattering rates due to electron–phonon (Fröhlich) interaction is of great practical interest, especially for the understanding of electrical transport properties in quantum wells such as phonon-assisted tunnelling [7]. Another important mechanism, apparently mediated by phonons, is the sweep-out of carriers in multiple quantum wells [8].

Ferreira and Bastard [9] have presented results using bulk phonons in single and double QWs under the influence of an electric field. Goodnick *et al* [10] used an

† Electronic address: gweber@brufmg (Bitnet)

0953-8984/92/499831+12$07.50 © 1992 IOP Publishing Ltd

ensemble Monte Carlo simulation to study relaxation in coupled QWs. Tang *et al* [11] calculated the resonant Raman profiles for superlattices using the Huang and Zhu model [12] and found that the phonon parity selection rules break down when an electric field is applied. Recently, Turley and Teitsworth [13, 14] presented a numerical calculation of electron–confined-phonon [13] and electron–IF-phonon [14] matrix elements in order to obtain resonant tunnelling currents. We have presented a calculation of scattering rates due to confined-phonon modes in quantum wells subjected to a longitudinal electric field [15]. We made a comparative study of the several dielectric continuum theory models currently under debate and found that the use of an electric field enhances the differences between the various models. For a more detailed discussion of the theories of confined-phonon modes we refer the reader to the excellent review by Menéndez [16]. Other reviews of interest are by Klein [17] and Cardona [18].

In this paper we present a calculation of scattering rates due to IF phonons in single quantum wells under the influence of an applied longitudinal electric field. We use the Hamiltonian as derived by Mori and Ando [19] and the electron wavefunctions are obtained by a variational approach as proposed by Bastard *et al* [20]. We show also results of scattering rates due to confined phonons (modified Huang and Zhu model) for GaAs–AlAs quantum wells and compare them with results for IF phonons. The scattering rates for confined phonons in these structures were obtained as in [15].

The paper is organized as follows, section 2 presents the Hamiltonian of the electron–IF-phonon interaction and the variational method which leads to the electron wavefunction under the influence of an electric field. In section 3 we present and discuss our results and in section 4 we draw our conclusions. In appendix A we present the analytical equations of the form factors for IF phonons.

2. Theory

For the description of the electron–IF-phonon Hamiltonian we follow strictly the work by Mori and Ando [19], which is largely equivalent to other descriptions such as those in Licari and Evrard [21], and Lassnig [22].

It is agreed [4, 23] that the IF phonons are reasonably well described within the framework of the slab model. As opposed to the confined-phonon modes in the slab model, the IF phonons are not dispersionless: two modes of different parity are identified as symmetric and antisymmetric modes, and for each of these modes there are two modes of different frequency for an interface like GaAs–AlAs. The energy dispersion with the parallel component of the phonon wavevector is given as [19]

$$\epsilon_W(\omega)\tanh(q_{||}L/2) + \epsilon_B(\omega) = 0 \tag{2.1a}$$

$$\epsilon_W(\omega)\coth(q_{||}L/2) + \epsilon_B(\omega) = 0 \tag{2.1b}$$

where equation (2.1*a*) ((2.1*b*)) is for symmetric (antisymmetric) modes, and $\epsilon_W(\omega)$ ($\epsilon_B(\omega)$) is the dielectric function of the well (barrier). Solving equations (2.1*a*, *b*) for a GaAs–AlAs QW we obtain two solutions for each parity, one with frequencies lying in the limit of GaAs bulk phonon frequencies and the other in the limit of AlAs bulk TO (transverse optical) and LO (longitudinal optical) phonon frequencies, therefore frequently referred to as GaAs-like and AlAs-like IF-phonon modes, respectively.

The electron–phonon Hamiltonian for IF phonons is [19]

$$H_{\alpha\mu} = \sum_{q_\parallel} \left(\frac{\omega_{\alpha\mu} e^2}{2\hbar A} \right)^{1/2} f_{\alpha\mu}(q_\parallel) h_\alpha(q_\parallel, z) \frac{e^{iq_\parallel \cdot r_\parallel}}{\sqrt{2q_\parallel}} [a_{\alpha\mu}(q_\parallel) + a^\dagger_{\alpha\mu}(-q_\parallel)] \tag{2.2}$$

where $\omega_{\alpha\mu}$ is the IF phonon frequency, $q_\parallel$ is the parallel component of the phonon wavevector, and $a_{\alpha\mu}$ and $a^\dagger_{\alpha\mu}$ are phonon creation and annihilation operators. The subscript α refers to the parity (S or A, signifying symmetric or antisymmetric respectively) and μ to the possible solutions of equations (2.1*a*, *b*), in our case to GaAs- and AlAs-like modes.

We also define the auxiliary functions

$$\beta_m(\omega) = \left(\frac{1}{\epsilon_{\infty m}} - \frac{1}{\epsilon_{0m}} \right) \frac{\omega^2_{\mathrm{LO}m}}{\omega^2} \left(\frac{\omega^2 - \omega^2_{\mathrm{TO}m}}{\omega^2_{\mathrm{LO}m} - \omega_{\mathrm{TO}m}} \right)^2 \tag{2.3}$$

and

$$f_{\mathrm{S}\mu}(q_\parallel) = [\beta_{\mathrm{W}}^{-1}(\omega_{\mathrm{S}\mu}) \tanh(q_\parallel L/2) + \beta_{\mathrm{B}}^{-1}(\omega_{\mathrm{S}\mu})]^{-1} \tag{2.4a}$$

$$f_{\mathrm{A}\mu}(q_\parallel) = [\beta_{\mathrm{W}}^{-1}(\omega_{\mathrm{A}\mu}) \coth(q_\parallel L/2) + \beta_{\mathrm{B}}^{-1}(\omega_{\mathrm{A}\mu})]^{-1} \tag{2.4b}$$

where m may be B (barrier) or W (well), ϵ_{0m} and $\epsilon_{\infty m}$ are the static and high-frequency dielectric constants, respectively.

The z-dependent part of the Hamiltonian is given by

$$h_{\mathrm{S}}(q_\parallel, z) = \begin{cases} e^{q_\parallel (z + L/2)} & z \leqslant -L/2 \\ \cosh(q_\parallel z)/\cosh(q_\parallel L/2) & |z| < L/2 \\ e^{-q_\parallel (z - L/2)} & z \geqslant L/2 \end{cases} \tag{2.5a}$$

$$h_{\mathrm{A}}(q_\parallel, z) = \begin{cases} e^{-q_\parallel (z + L/2)} & z \leqslant -L/2 \\ \sinh(q_\parallel z)/\sinh(q_\parallel L/2) & |z| < L/2 \\ e^{-q_\parallel (z - L/2)} & z \geqslant L/2 \end{cases} . \tag{2.5b}$$

For the description of the electron envelope wavefunction of the ith confined subband we use a variational method proposed by Bastard *et al* [20], instead of an exact solution expressed in terms of Airy functions. It is well known that the variational approach yields excellent results [24] and is more suitable for the calculation of intra- and intersubband transition matrix elements because all integrals can be carried out analytically.

Assuming the usual effective-mass approximation for the conduction band and a finite barrier height V_{B}, the envelope wavefunction for the electron in the ith conduction subband is [20]

$$\psi_i(z) = b_i \begin{cases} \alpha_i^- \exp[k_{\mathrm{B}i}(z + L/2)] e^{-\beta z} & z \leqslant -L/2 \\ \sin(k_{\mathrm{W}i} z + \delta_i) e^{-\beta z} & |z| < L/2 \\ \alpha_i^+ \exp[-k_{\mathrm{B}i}(z - L/2)] e^{-\beta z} & z \geqslant L/2 \end{cases} \tag{2.6}$$

where

$$k_{Bi} = [2m^*(V_b - E_i^0)]^{1/2}/\hbar \qquad k_{Wi} = (2m^* E_i^0)^{1/2}/\hbar \tag{2.7}$$

with E_i^0 being the ith unperturbed energy level, and

$$\alpha_i^{\pm} = \sin(\delta_i \pm k_{Wi} L/2) \tag{2.8}$$

b_i is a normalization constant, and β is the variational parameter. For the first two subbands the values of δ_i are $\delta_1 = \pi/2$ and $\delta_2 = 0$. For simplicity, the effective mass m^* of the barrier is assumed to be the same as that of the well. In order to obtain the energy levels with an applied electric field we evaluate the matrix elements of the Hamiltonian,

$$H_0 = -(\hbar^2/2m^*)(\partial^2/\partial z^2) + V(z) + |e|Fz \tag{2.9}$$

where $V(z)$ is the finite QW potential and F the strength of the applied electric field. Finally, the energy levels $E_i(F,\beta) = \langle\psi_i|H_0|\psi_i\rangle$ are minimized numerically with respect to the variational parameter β [20].

The scattering rates for the emission of a IF phonon with energy $\hbar\omega_{\alpha\mu}$ are obtained from the usual Fermi golden rule

$$W_{\alpha\mu}^{(i\to f)}(k_{\|i}) = \frac{2\pi}{\hbar}\int \delta(\mathcal{E}_i - \mathcal{E}_f - \hbar\omega_{\alpha\mu})|\langle \boldsymbol{k}_f|H_{\alpha\mu}|\boldsymbol{k}_i\rangle|^2 \,\mathrm{d}N_f \tag{2.10}$$

where $\mathcal{E}$ is the total electron energy, i.e.

$$\mathcal{E} = \hbar^2 k_{\|}^2/2m^* + \hbar^2 k_z^2/2m^* = \hbar^2 k_{\|}^2/2m^* + E. \tag{2.11}$$

Evaluating the matrix element in equation (2.10) with the Hamiltonian given by equation (2.2) we obtain the expression for the scattering rates,

$$W_{\alpha\mu}^{(i\to f)}(Q) = (e^2 m^*/4\hbar^4)(\omega_{\alpha\mu} f_{\alpha\mu}/Q)(N_q + 1)|G_{\alpha\mu}^{(i\to f)}(Q)|^2 \tag{2.12}$$

where $G_{\alpha\mu}^{(i\to f)}(Q)$ is the overlap integral of the electron wavefunction and the z-dependent part of the electron–IF-phonon Hamiltonian,

$$G_{\alpha\mu}^{(i\to f)}(Q) = \int_{-\infty}^{\infty} \psi_f^*(z) h_\alpha(q_{\|}, z)\psi(z)_i \,\mathrm{d}z. \tag{2.13}$$

For details on the analytical form of equation (2.13) see appendix A. For intrasubband $(1 \to 1)$ transitions, such that the electron has initially just enough energy to emit one phonon with frequency $\omega_{\alpha\mu}$, Q is given as

$$Q = [2m^*\omega_{\alpha\mu}(q_{\|})/\hbar]^{1/2} \tag{2.14a}$$

and for intersubband $(2 \to 1)$ transitions

$$Q = \left\{2m^*[E_i - E_f - \hbar\omega_{\alpha\mu}(q_{\|})]/\hbar\right\}^{1/2} \tag{2.14b}$$

where we take the electron to be initially at the bottom of the second subband. Notice that we are not neglecting the phonon dispersion for the calculation of scattering rates as was done by Rudin and Reinecke [25]; the appropriate values of $\omega_{\alpha\mu}$ and $q_{\|}$ are calculated for each case.

3. Results and discussion

For the calculation of scattering rates due to IF phonons we assume always a GaAs–AlAs QW with a finite barrier of 1 eV. The material parameters used in our calculations are: for GaAs, the effective mass $m^* = 0.0665$, the dielectric constants $\epsilon_0 = 12.35$ and $\epsilon_\infty = 10.48$, the bulk phonon energies $\hbar\omega_{LO} = 36.8$ meV and $\hbar\omega_{TO} = 34.0$ meV; for AlAs, the effective mass is assumed to be the same as for GaAs, the dielectric constants $\epsilon_0 = 10.0$ and $\epsilon_\infty = 8.16$, the bulk phonon energies $\hbar\omega_{LO} = 47.7$ meV and $\hbar\omega_{TO} = 44.0$ meV.

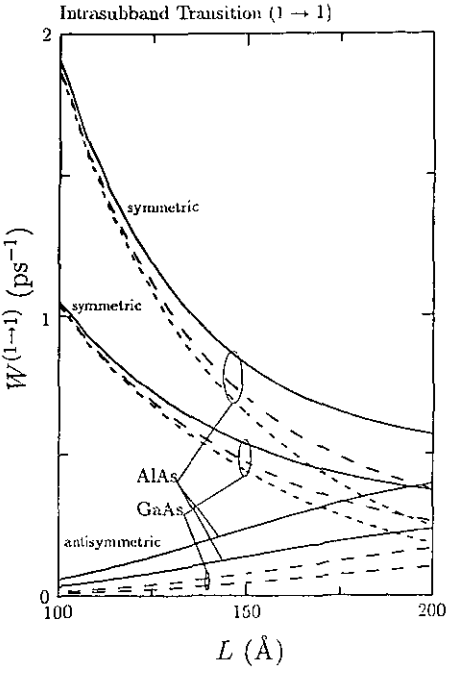

Figure 1. Intrasubband ($1 \rightarrow 1$) scattering rates due to IF phonons in a GaAs–AlAs quantum well, as a function of the quantum well width L. The full curve is for an electric field of 100 kV cm^{-1}, the long broken curve is for 50 kV cm^{-1} and the short broken curve is for the absence of an electric field. The indication 'GaAs' ('AlAs') stands for GaAs-like (AlAs-like) IF-phonon modes.

In figure 1 we show the scattering rates for intrasubband transitions ($1 \rightarrow 1$) due to IF phonons in GaAs–AlAs QWs *a uniform electric field of 50* kV cm^{-1}, *100* kV cm^{-1} and in the absence of an electric field. Note that the antisymmetric IF modes now contribute to the scattering and these scattering rates become significant for large QWs (about 200 Å), as opposed to the rate without an applied electric field.

Intersubband ($2 \rightarrow 1$) transitions rates, shown in figure 2, present a much stronger dependence with the applied electric field (50 kV cm^{-1}) than intrasubband scattering rates, although significant changes to the zero-field cases are observed only for QWs larger than 100 Å. Now the contribution from the previously inactive symmetric modes not only increases with increasing electric field but also the scattering rate due to symmetric AlAs-like mode becomes even *higher* than the scattering rates due to the antisymmetric AlAs-like mode. We observe a maximum scattering rate of 15.6 ps^{-1} (off scale in figure 2 for a QW of 158 Å, which corresponds to a scattering time of 64 fs.

In general, the scattering rates due to IF modes increase with the strength of the applied electric field. This is in contrast to confined phonons where the intrasubband

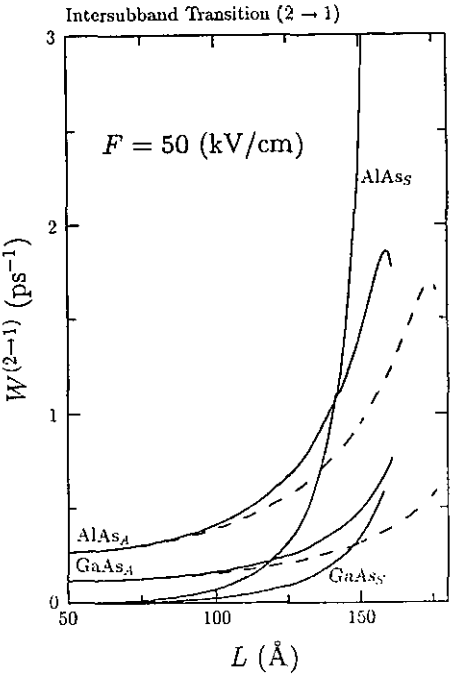

Figure 2. Intersubband (2 → 1) scattering rates due to IF phonons in a GaAs–AlAs quantum well, as a function of the quantum well width L. The full curve is for an electric field of 50 kV cm^{-1} and the broken curve is for the absence of an electric field. The indication 'GaAs' ('AlAs') stands for GaAs-like (AlAs-like) IF-phonon modes. The subscripts S and A signify symmetric and antisymmetric modes, respectively. The scattering rate for the symmetric AlAs-like mode reaches a maximum of 15.6 ps^{-1} (off scale in the figure) for a QW of 158 Å.

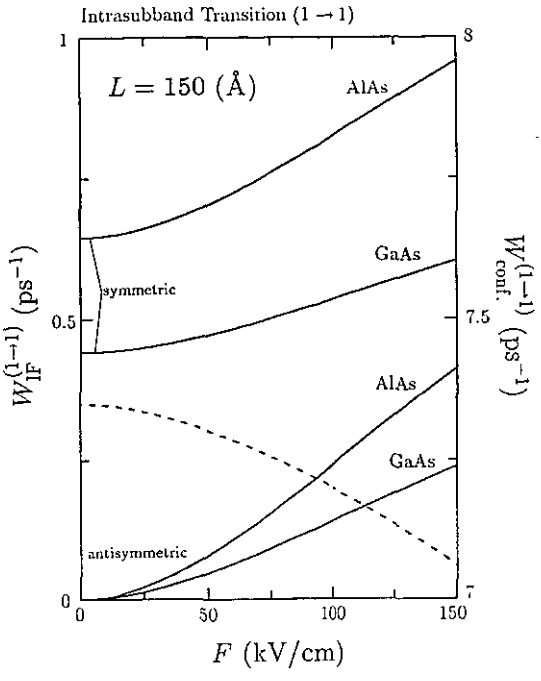

Figure 3. Intrasubband (1 → 1) scattering rates due to IF phonons in a GaAs–AlAs quantum well of L = 150 Å, as a function of the applied longitudinal electric field F. For comparison, we also show the scattering rates due to confined phonons (broken curve; modified Huang and Zhu model) calculated as in [15]. Notice that the scales for IF and confined phonons are different but proportional in order to compare the variation with the electric field directly. The indication 'GaAs' ('AlAs') stands for GaAs-like (AlAs-like) IF phonon modes.

scattering rates *decrease*, whereas the intersubband rates increase with the electric field.

In figure 3 we show the electric-field dependence of the intrasubband (1 → 1) scattering rates for a GaAs–AlAs QW of 150 Å, i.e. large enough to observe significant changes in scattering rates. Above 50 kV cm^{-1} the increase in scattering rates is almost linear with respect to the electric-field strength. In this figure we included the scattering rates due to GaAs confined-phonon modes (modified Huang and Zhu model [12, 25]) calculated as in [15].

For the intersubband (2 → 1) transitions, shown in figure 4 as a function of the electric field, we notice that the symmetric modes (which are inactive at zero electric field) present stronger variations with the electric field than their respective antisymmetric modes. In figure 4(*b*) we observe the very interesting case of the scattering rate due to AlAs-like symmetric modes becoming *higher* than the rates due to confined modes in QWs of 150 Å at fields stronger than 50 kV cm^{-1} and reaching a maximum of 34 ps^{-1} (off scale in figure 4(*b*)) at a field of 84 kV cm^{-1}. This

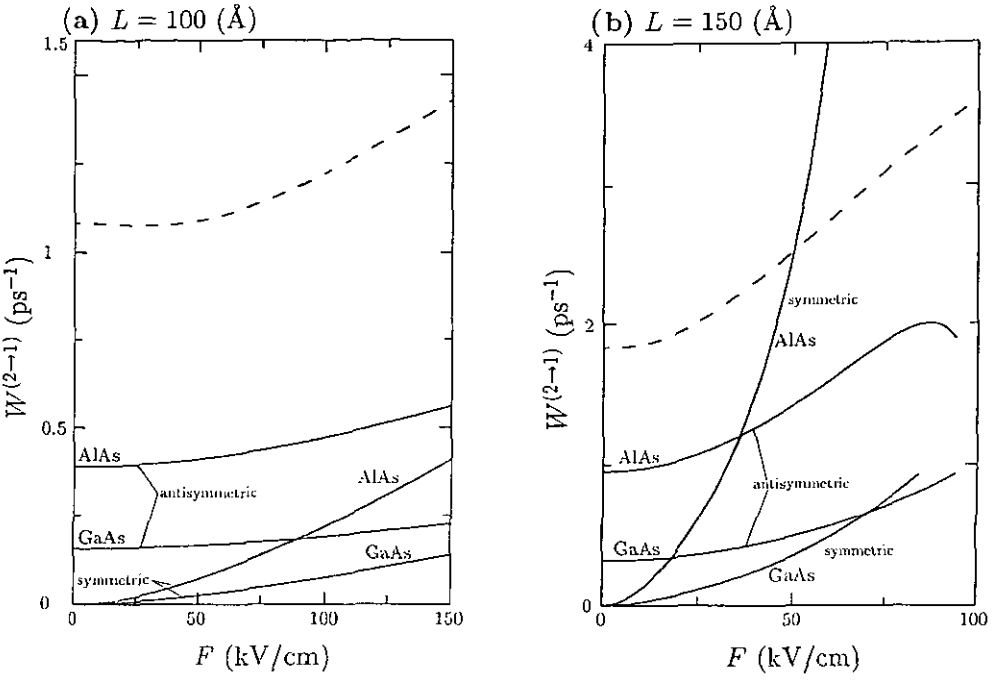

Figure 4. Intersubband ($2 \to 1$) scattering rates due to IF phonons in a GaAs–AlAs QW of (*a*) $L = 100$ Å and (*b*) $L = 150$ Å, as a function of the applied longitudinal electric field F. For comparison, we show the scattering rates due to confined phonons (broken curve; modified Huang and Zhu model) calculated as in [15]. In part (*b*) the scattering rate for the symmetric AlAs-like mode has a maximum of 34 ps^{-1} (off scale in the figure) at an electric field of 84 kV cm^{-1}. The indication 'GaAs' ('AlAs') stands for GaAs-like (AlAs-like) IF-phonon modes.

corresponds to a maximum scattering time of ≈ 30 fs.

This effect should be observable in experimental measurements, especially those involving time-resolved optical techniques [26–29]. This is a promising propect; calculations of electron–phonon scattering rates using the dielectric continuum model seem to be sufficiently accurate, despite obvious limitations, and they reproduce experimental measurements quite well [30, 31].

In figure 5 we show the IF phonon energies obtained for the lowest possible Q (see equation (2.14*b*)) in an intersubband transition as a function of the width of the QW, which were used for the calculation of the scattering rates presented in figure 2. These results show a non-negligible shift in energy of the AlAs-like modes for sufficiently large QWs. The largest shift is for a QW of 158 Å, where a shift in AlAs-like symmetric modes of about 0.6 meV was calculated. Although this shift will depend also on the electron excess energy (we are always using the lowest possible energy for an intersubband transition), these results suggest an experimentally observable energy shift caused by a longitudinal electric field. Note that the fast decrease of the IF phonon energy for AlAs-like antisymmetric modes explains the peak in the intersubband scattering rates (figure 2) for large QWs, as the scattering rate is proportional to the phonon energy (see equation (2.12)).

So far we have presented our results for the scattering rates due to IF phonon

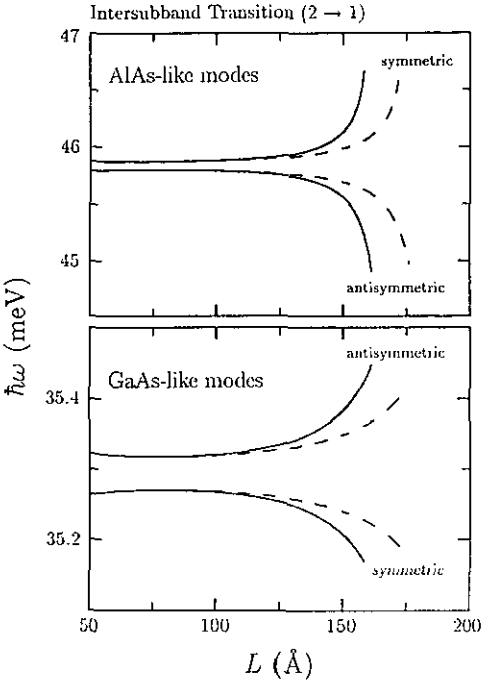

Figure 5. IF-phonon energies as functions of the QW width L, as used for the calculation of intersubband $(2 \rightarrow 1)$ transition scattering rates in figure 2. The full curve is for an electric field of 50 kV cm^{-1} and the broken curve is for the absence of an electric field. The zero-electric field symmetric frequencies are shown only for comparison, they are otherwise meaningless as there are no intersubband transitions due to symmetric IF-phonon modes in the absence of an electric field. Although IF modes at larger QWs are possible, we show only those who participate in the intersubband transitions satisfying energy conservation.

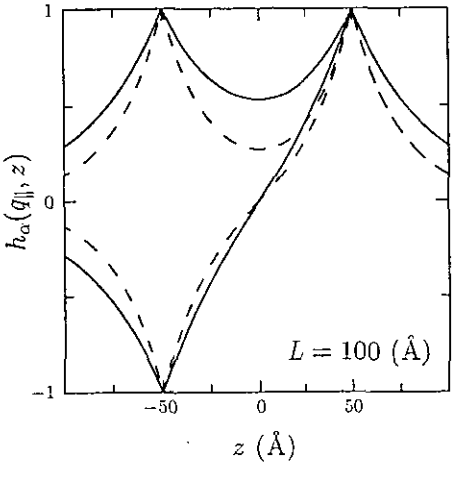

Figure 6. The z-dependent part of the electron–IF-phonon Hamiltonian (equations (2.5*a*, *b*)), as a function of the position in a QW of 100 Å. Full curves are for intrasubband transitions with $q_\parallel L = 2.5$, and broken curves are for intersubband transitions with $q_\parallel L = 4$.

modes in QWs subjected to an electric field, yet it remains to be understood why the intrasubband $(1 \rightarrow 1)$ scattering rates yield a relatively small variation. One might expect a more pronounced change in these scattering rates if we follow similar considerations as for confined modes [15]. In figure 6 we show the z-dependent part of the electron–IF-phonon Hamiltonian for a QW of 100 Å. It is apparent from this figure that there is a strong dependence on the phonon wavevector; for intrasubband transitions a typical value is $q_\parallel L = 2.5$ and for intersubband transitions $q_\parallel L = 4$. For intersubband $(2 \rightarrow 1)$ transitions the z-dependent part of the Hamiltonian is much more localized towards the interfaces and therefore more sensitive to the electric field; the variation relative to the intrasubband transitions is more pronounced for the symmetric modes. It can therefore be expected that the scattering rates due to symmetric IF modes present the largest variation with electric field for intersubband transitions and this is exactly the behaviour observed in our results (see figures 2 and 4).

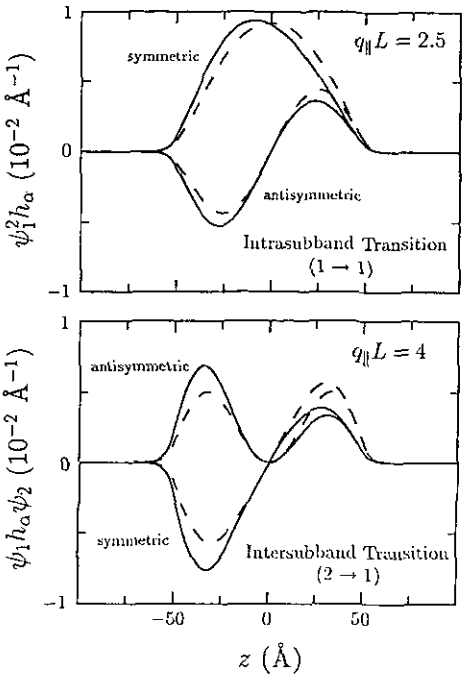

Figure 7. Overlap of the z-dependent part of the electron–IF-phonon Hamiltonian and the electric-field-dependent electron wavefunctions (integrand of equation (2.13)) as a function of the position in a QW of 100 Å. The upper (lower) figure is for intrasubband (intersubband) transitions. The full curve is for an electric field of 50 kV cm^{-1} and the broken curve is for the absence of an electric field. The remaining parameters are the same as for figure 6. The indications 'symmetric' and 'antisymmetric' refer to the parity of the z-dependent part of the electron–IF-phonon Hamiltonian.

Going further, we show in figure 7 the overlap of the electronic wavefunctions and the z-dependent part of the Hamiltonian which shows clearly that the integral of the overlap, i.e. $G_{\alpha\mu}^{(i\rightarrow f)}(Q)$, will not be very sensitive to the electric field for intrasubband transitions. In contrast, for intersubband transitions the effect is much more pronounced for symmetric IF-phonon modes than for antisymmetric modes.

Another consequence which results from the inspection of figures 6 and 7 is that the scattering rates have a strong dependence on the IF-phonon dispersion. Therefore, simply replacing $q_\parallel L$ by an asymptotic value of ~ 3 as proposed by Rudin and Reinecke [25] would not be appropriate.

4. Conclusions

We have presented a calculation of scattering rates for intrasubband and intersubband transitions mediated by IF-phonon modes in QWs, when subjected to a longitudinal electric field. It is found that the usual selection rules break down and that the scattering rates always increase with the applied electric field, in contrast to scattering rates due to confined-phonon modes which decrease for intrasubband transitions [15].

In particular we found very high intersubband scattering rates for large QW which becomes the dominant scattering mechanism at sufficiently large QWs. We may conclude that in applying a longitudinal electric field to large QWs it may be possible to achieve scattering times which are up to one order of magnitude faster. This certainly has important consequences for device applications where the electron–phonon interaction is an important mechanism.

Although specific experimental measurements on this subject are, to the best of our knowledge, not yet available, we hope that our calculations may motivate experimental studies on electron–phonon interaction in QWs subjected to longitudinal electric fields.

Acknowledgments

We are grateful to A M de Paula for helpful discussions and for the critical reading of this manuscript. Financial support by Conselho Nacional de Desenvolvimento Científico e Tecnológico (CNPq, Brazil) is acknowledged.

Appendix A. Form factors for IF phonons

We define the auxiliary functions

$$g_{\pm}(\beta) = \{L[-(\beta L - q_{\|} L/2)\sin k_{W\pm} L\cosh(\beta L - q_{\|} L/2) + k_{W\pm} L\cos k_{W\pm} L\sinh(\beta L - q_{\|} L/2)]\}[(\beta L - q_{\|} L/2)^2 + (k_{W\pm} L)^2]^{-1} \tag{A1}$$

$$h_{\pm}(\beta) = \{L[-(\beta L + q_{\|} L/2)\sin k_{W\pm} L\cosh(\beta L + q_{\|} L/2) + k_{W\pm} L\cos k_{W\pm} L\sinh(\beta L + q_{\|} L/2)]\}[(\beta L + q_{\|} L/2)^2 + (k_{W\pm} L)^2]^{-1} \tag{A2}$$

$$i_{\pm}(\beta) = \{L[(\beta L - q_{\|} L/2)\cos k_{W\pm} L\sinh(\beta L - q_{\|} L/2) + k_{W\pm} L\sin k_{W\pm} L\cosh(\beta L + q_{\|} L/2)]\}[(\beta L - q_{\|} L/2)^2 + (k_{W\pm} L)^2]^{-1} \tag{A3}$$

$$j_{\pm}(\beta) = \{L[(\beta L + q_{\|} L/2)\cos k_{W\pm} L\sinh(\beta L + q_{\|} L/2) + k_{W\pm} L\sin k_{W\pm} L\cosh(\beta L + q_{\|} L/2)]\}[(\beta L + q_{\|} L/2)^2 + (k_{W\pm} L)^2]^{-1} \tag{A4}$$

$$k_{W\pm} = (k_{Wf} \pm k_{Wi})/2 \qquad \delta_{\pm} = (\delta_f \pm \delta_i)/2. \tag{A5}$$

The form factor as obtained from equation (2.13) is

$$G_S^{(i\to f)}(Q) = b^2\left(\frac{L}{2}\frac{(\alpha^-)^2 e^{\beta L}}{(k_B L - \beta L + q_{\|} L/2)} + \frac{L}{2}\frac{(\alpha^+)^2 e^{-\beta L}}{(k_B L + \beta L + q_{\|} L/2)} + \frac{1}{4\cosh q_{\|} L/2}\sum_{\pm}[\pm\sin 2\delta_{\pm}(g_{\pm} + h_{\pm}) \mp \cos 2\delta_{\pm}(i_{\pm} + j_{\pm})]\right) \tag{A6}$$

for symmetric IF-phonon modes, and

$$G_{\mathrm{A}}^{(\mathrm{i}\to\mathrm{f})}(Q) = b^2\left(-\frac{L}{2}\frac{(\alpha^-)^2\mathrm{e}^{\beta L}}{(k_{\mathrm{B}}L-\beta L+q_{\|}L/2)}+\frac{L}{2}\frac{(\alpha^+)^2\mathrm{e}^{-\beta L}}{(k_{\mathrm{B}}L+\beta L+q_{\|}L/2)}\right.$$
$$\left.+\frac{1}{4\cosh q_{\|}L/2}\sum_{\pm}[\pm\sin 2\delta_{\pm}(g_{\pm}-h_{\pm})\mp\cos 2\delta_{\pm}(i_{\pm}-j_{\pm})]\right) \qquad \text{(A7)}$$

for antisymmetric modes. For intra- and intersubband transitions Q is given by equations (2.14*a*) and (2.14*b*), respectively.

References

[1] Sood A K, Menéndez J, Cardona M and Ploog K 1985 *Phys. Rev. Lett.* **54** 2115
[2] Lambin P, Vigneron J P, Lucas A A, Thiry P A, Liehr M, Pireaux J J, Caudano R and Kuech T 1986 *Phys. Rev. Lett.* **56** 1842
[3] Maciel A C, Cruz L C C and Ryan J F 1987 *J. Phys. C: Solid State Phys.* **20** 3041
[4] Arora A K, Ramdas A K, Melloch M R and Otsuka N 1987 *Phys. Rev.* B **36** 1021
[5] Meynadier M H, Finkman E, Sturge M D, Worlock J M and Tamargo M C 1987 *Phys. Rev.* B **35** 2517
Gant T A, Delaney M, Klein M V, Houdré R and Morkoç H 1989 *Phys. Rev.* B **39** 1696
Fuchs H D, Mowbray D J, Cardona M, Chalmers S A and Gossard A C 1991 *Solid State Commun.* **79** 223
Huber A, Egeler T, Ettmüller W, Rothfritz H, Tränckle G and Abstreiter G 1991 *Superlatt. Microstruct.* **9** 309
Tsen K T, Smith D J, Tsen S C Y, Kumar N S and Morkoç H 1991 *J. Appl. Phys.* **70** 418
Wang Z P, Han H X, Li G H, Jiang D S and Ploog K 1992 *J. Phys.: Condens. Matter* **4** 367
[6] Schwartz G P, Gualtieri G J, Sunder W A and Farrow L A 1987 *Phys. Rev.* B **36** 4868
[7] Goldman V J, Tsui D C and Cunningham J E 1987 *Phys. Rev.* B **36** 7635
Shorthose M G, Ryan J F and Moseley A 1989 *Solid-State Electron.* **32** 1449
Oberli D V, Shah J, Damen T C, Kuo J M, Henry J E, Lary J and Goodnick S M 1990 *Appl. Phys. Lett.* **56** 1239
Muto S, Inata T, Tackeuchi A, Sugiyama Y and Fuji T 1991 *Appl. Phys. Lett.* **58** 2393
[8] Fox A M, Miller D A B, Livescu G, Cunningham J E and Jan W Y 1991 *Quantum Optoelectronics (Technical Digest 7)* (Optical Society of America) pp 260–3
[9] Ferreira R and Bastard G 1988 *Phys. Rev.* B **40** 1074
[10] Goodnick S M, Lary J E and Lugli P 1990 *Proc. SPIE* **1283** 175
[11] Tang H, Zhu B and Huang K 1990 *Phys. Rev.* B **42** 3082
[12] Huang K and Zhu B 1988 *Phys. Rev.* B **38** 13377
[13] Turley P J and Teitsworth S W 1991 *Phys. Rev.* B **44** 3199
[14] Turley P J and Teitsworth S W 1991 *Phys. Rev.* B **44** 8181
[15] Weber G and Ryan J F 1992 *Phys. Rev.* B to be published
[16] Menéndez J 1989 *J. Lumin.* **44** 285
[17] Klein M V 1986 *IEEE J. Quantum Electron.* **QE-22** 1760
[18] Cardona M 1989 *Superlat. Microstruct.* **5** 27
[19] Mori N and Ando T 1989 *Phys. Rev.* B **40** 6175
[20] Bastard G, Mendez E E, Chang L L and Esaki L 1983 *Phys. Rev.* B **28** 3241
[21] Licari J J and Evrard R 1977 *Phys. Rev.* B **15** 2254
[22] Lassnig R 1984 *Phys. Rev.* B **30** 7132
[23] Rücker H, Molinari E and Lugli P 1991 *Phys. Rev.* B **44** 3463; 1991 *Phys. Rev.* **45** 6747
[24] Weber G 1990 *Phys. Rev.* B **41** 10043, and references therein
[25] Rudin S and Reinecke T L 1990 *Phys. Rev.* B **41** 7713; 1990 *Phys. Rev.* B **43** 9298(E)
[26] von der Linde D, Kuhl J and Klingenberg H 1980 *Phys. Rev. Lett.* **44** 1505
[27] Tatham M C, Ryan J F and Foxon C T 1989 *Phys. Rev. Lett.* **63** 1637

[28] de Paula A M, Maciel A C, Tatham M C, Ryan J F, Dawson P and Foxon C T 1990 *Proc. 20th Int. Conf. on the Physics of Semiconductors (Thessaloniki, Greece 1990)* vol 2, ed E M Anastassakis and J D Joannopuolos (Singapore: World Scientific) pp 1421–4

[29] de Paula A M, Maciel A C, Weber G, Ryan J F, Dawson P and Foxon C T 1992 *Semicond. Sci. Technol.* B 7 120

[30] Jain J K and Das Sarma S 1989 *Phys. Rev. Lett.* **62** 2305

[31] Weber G, de Paula A M and Ryan J F 1991 *Semicond. Sci. Technol.* **6** 397